APPLIED CHEMISTRY

Formation of Solid Sulfur by Decomposition of Carbon Disulfide in the Oxygen-Lean Cold Plasma Environment

Cheng-Hsien Tsai,[†] Wen-Jhy Lee,*[,†] Chuh-Yung Chen,[‡] Wei-Tung Liao,[†] and Minliang Shih[†]

Departments of Environmental Engineering and Chemical Engineering, National Cheng Kung University, Tainan 70101, Taiwan

In general, the conventional thermal processes for treating toxic carbon disulfide (CS_2) gas were by the oxidation of sulfur on CS_2 to form SO_2. However, this study demonstrated that by using a radio-frequency cold plasma reactor in the oxygen-lean condition ($O_2/CS_2 = R = 0.6$) at the applied power of 90 W, the decomposition fraction of CS_2 could reach 88.2%, and there was 76.9% of input sulfur mass from CS_2 converted into solid sulfur with the purity of 99.2%. No solid sulfur was observed for the no-oxygen ($R = 0$) or oxygen-rich conditions ($R = 3.0$). Hence, the results of this study provided an approach for sulfur recovery to reduce the emissions of both CS_2 and SO_2. In addition, the reaction mechanisms for the decomposition of CS_2 and for the formation of gaseous SO_2, CO, CO_2, and OCS in the CS_2/O_2/Ar plasma were also built up and discussed.

1. Introduction

Carbon disulfide (CS_2) is an odorous organic sulfur compound with the olfactory detection threshold of approximately 0.21 ppm. For natural emissions, CS_2 is present in surface open ocean waters and has been estimated at 1.03×10^7 mol/day of oceanic flux to contribute about 3% on a global scale, that is, approximately 1.13×10^6 mol/day from terrestrial sulfur fluxes.[1] Therefore, CS_2 is a natural component of the troposphere, and it has been observed at elevated levels in the polluted troposphere.[2] Oxidation of CS_2 may produce carbonyl sulfide (OCS), which has a half-life of several years.[2]

In industry, a large amount of exhaust air contaminated with CS_2 is generated in the traditional processes of cellophane, rayon, and carbon tetrachloride, and the concentration for gas in air can reach as high as 2 g/m^3.[3] CS_2 has been classified in the U.S. as a hazardous air pollutant in Title III of the Clean Air Act Amendments of 1990 and is considered to be one of most toxic solvents, causing accelerated atherosclerosis and coronary artery disease for those exposed to it in poorly ventilated factories.[4]

Combustion, biological gas desulfurization processes, or catalyst oxidation could be adopted to treat CS_2. The main products were SO_2 and CO with small amounts of CO_2 and OCS for either a 80 °C cool flame or combustion at 927 °C and H_2SO_4 for biological treatment, respectively.[3,5] Recently, the trends toward the development to destroy hazardous air pollutants by using radio-frequency (RF; 13.56 MHz) plasma technologies were also proposed. It has been successfully applied to decompose 1,1-$C_2H_2Cl_2$, CH_2Cl_2, CH_3Cl, CCl_2F_2, CHF_3, ethoxyethane, and ethylene oxide.[6−11] Other plasmas were also used to treat odorous gases such as NH_3, H_2S, and SO_2.[12−15]

A 13.56 MHz RF source is commonly used in industry and is called cold plasma because its electrons have greater temperature and kinetic energy than those of ions and neutral molecules.[16] Therefore, the conventional reactions needed to be achieved at a higher activation energy can now be done at a relatively lower gas temperature in the RF plasma system to avoid the problems caused by high temperature of combustion or catalyst poisons.[17]

For CS_2 in the reductive tail gas, the sulfur can be reconverted by the redox Claus reaction but must be hydrolyzed to H_2S first[18] while the feasibility of solid sulfur recovery by using the RF plasma process at different operational conditions has not been extensively studied yet. However, sulfur recovery with the solid state has the advantage of gas volume reduction by approximately a factor of 1000. On the other hand, high-pressure polymerization,[19,20] chemical polymerization,[21] photolysis,[22] laser-induced polymerization,[23−25] and plasma polymerization[26−28] of CS_2 usually led to the formation of dark brown to black depositions or polymers.

In this study, the formation of solid sulfur by decomposition of CS_2 in an RF plasma reactor was investigated. In addition, the reaction mechanisms for decomposition of CS_2 and for the formation of SO_2, CO, CO_2, OCS, and polysulfur in the CS_2/O_2/Ar plasma were also built up and discussed in this study.

2. Experimental Section

The operation conditions were the applied RF power (E) in the range between 15 and 90 W, the O_2/CS_2 ratio

* Corresponding author. E-mail: wjlee@mail.ncku.edu.tw.
[†]Department of Environmental Engineering.
[‡]Department of Chemical Engineering.

10.1021/ie010292s CCC: $22.00
Published on Web 02/21/2002

(R) between 0 and 3.0, and the operating pressure at 30 Torr at a constant total gas flow rate of 100 sccm with 5% of CS_2 (0.223×10^{-3} mol/min). The yields of gaseous product were based on the mole fraction of the effluent gas stream.

2.1. Experimental Apparatus. The experimental apparatus and flowcharts have been described in detail elsewhere.[6−11] In short, the flow rates of CS_2, O_2, and Ar gas were adjusted with calibrated mass flow controllers (Sierra series 820 and Brooks 5850 E), respectively, and then mixed and introduced into a vertical cylindrical glass reactor (4.14 cm i.d. × 15 cm height). The plasma reactor was wrapped in two outer copper electrodes coupled to a 13.56 MHz, 0−500 W RF generator (PFG 600 RF, Fritz Huttinger Elektronik Gmbh) with a matching network (Matchbox PFM) to generate a glow discharge.

To clean up the contaminants and check the leak for the overall system, the pressure of the system was kept lower than 10^{-3} Torr by a mechanical vacuum pump (Pfeiffer DUO 065 DC) with a diffusion oil pump until a new experiment was performed. Each designed experimental condition was achieved by measuring the concentration of the reactants and products at least three times to ensure that the plasmachemical reactions were in the steady state.

2.2. Chemical Analysis. The gaseous products were identified by a gas chromatograph (GC) equipped with a pulsed flame photometric detector (GC/PFPD, HP 6890, GSQ column, 30 m × 0.53 mm) and a Fourier transform infrared spectrometer (FTIR; Bio-Rad, FTS-7) first and then quantified mainly by the on-line FTIR. GC aliquots from the effluent gas mixture were sampled through a canister sampler (6 L) from the outlet valve on the downstream of the reactor and then pressurized slightly to over 1000 Torr by adding pure N_2 gas. For FTIR, the analysis condition was at a resolution of 4 cm^{-1}, sensitivity = 1, and scan number = 8, and calibration curves of the reactants and products were achieved by withdrawing standard gas directly into the gas chamber. According to a comparison of the response peak height at the same IR wavenumber, a plot of absorbance versus concentration should give a straight line or curvature for each standard gas.

The solid samples called depositions in the major glow discharge zone and called clusters in the front of the glow discharge zone for the determination of chemical compositions were collected from the inner wall of the reactor and then analyzed by the elemental analyzers (elementar/vario EL for C, H, N, and S and Heraeus/CHN−O− rapid analyzer for O). The structures of these solid samples were determined by X-ray diffraction (XRD) spectroscopy (Rigaku model D/MAX III-V) with Cu Kα radiation that scanned from 5 to 80° (2θ) and a single-crystal X-ray diffractometer (SC-XRD).

In the rear of the glow discharge zone, trace amounts of plasma polymeric thin films were also collected by several pieces of copper plate that attached on the inner wall of the reactor. After cooling to the room temperature, these plate samples were conserved in a N_2 bag for further analyses. The surface analyses of the films were performed by X-ray photoelectron spectroscopy (XPS) measured on a Fison electron spectroscopy for chemical analysis (ESCA 210; VG Scientific) spectrometer with an Mg Kα X-ray (1253.6 eV) excitation source.

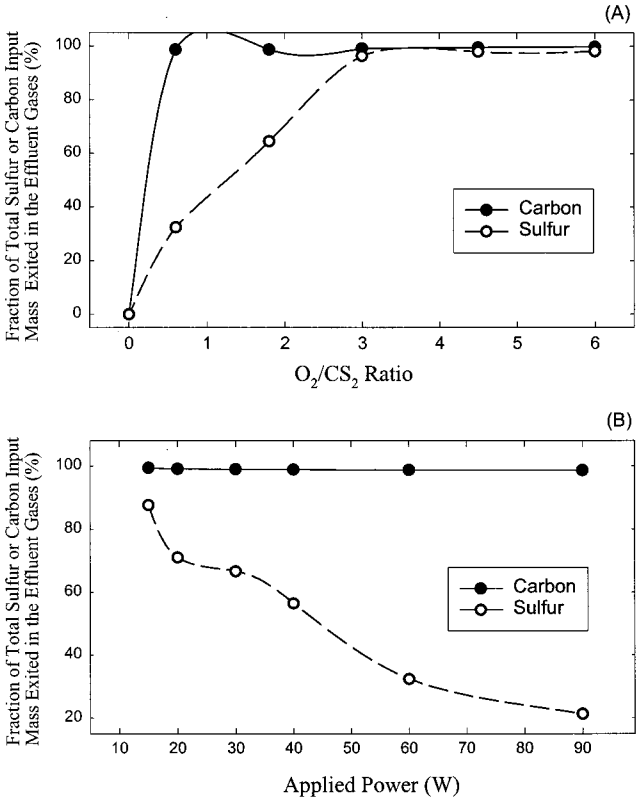

Figure 1. Fraction of total sulfur or carbon input mass exited in the effluent gases at $E = 60$ W under various O_2/CS_2 ratios (A) and at $R = 0.6$ under different applied powers (B).

3. Results and Discussion

The decomposition fractions of CS_2 (η_{CS_2}) and reaction products were studied under various applied RF powers (E) at various O_2/CS_2 ratios (R).

3.1. Decomposition of CS_2. Mass Balance and Sulfur Conversion. To understand the fraction of total sulfur input mass from CS_2 input being converted into solid products, the quantification data were checked through mass balances. Figure 1 shows that the fraction of total sulfur or carbon input mass from CS_2 exited in the effluent gases.

Figure 1A reveals that $R = 3$ was the critical ratio of O_2/CS_2 and the fraction of total sulfur input mass apparently decreased at the oxygen-lean conditions. At $R = 0$, no gaseous product was detected to lead to the fraction equal to zero. Therefore, to keep enough oxygen to remove C atoms by forming CO or CO_2 with a higher decomposition fraction of CS_2, the minimum O_2/CS_2 ratio was terminated at 0.6, which is a little greater than the stoichiometry coefficient of 0.5 for the reaction $CS_2 + 0.5O_2 \rightarrow CO + SO_2$. Besides, Figure 1B shows that the fraction of total sulfur input mass converted into effluent gases reduced significantly from 87.7% to 21.2% when E was increased from 15 to 90 W.

By comparison with the dissociation energy, the energy of C═O (257 kcal/mol) is much greater than those of O═O (119.2 kcal/mol) and SC═S (102.7 kcal/mol). Hence, at an oxygen-limiting condition, the higher thermodynamic stability of CO led to oxygen providing a prior sink for carbon atoms, mainly converting CS_2 into CO, while the majority of S atoms remained as polysulfur via heterogeneous wall reactions.

Decomposition Fraction of CS_2. Actually, it was difficult to decompose pure CS_2 in RF plasma; η_{CS_2} was only 9.2% at $E = 60$ W and 10.0% when E was elevated

up to 90 W. However, the addition of oxygen easily improved η_{CS_2}. Figure 2A shows that η_{CS_2} increased significantly from 24.8% to 88.2% at $R = 0.6$ and from 83.8% to 99.88% at $R = 3.0$ by increasing the applied power from 15 to 90 W to indicate that η_{CS_2} was more sensitive to the O_2/CS_2 ratio than to the applied power and exhibits a positive effect on η_{CS_2}.

The addition of O_2 not only elevated the probabilities of high activity species CS_2*, CS, or S being oxidized to improve the η_{CS_2} but also showed a much lesser tendency toward deposition of the solid. On the other hand, the elevated applied power caused the rise of the power density to result in the Maxwellian electron energy distribution function toward the elevation of the average electron temperature and hence an increase in the reaction rate for electron-impact-molecule dissociation reactions.[8,29]

Initial Reactions. The main initial reactions include the excitation and dissociation in the O_2/Ar plasma (eqs 1−3)[30] and the decomposition of CS_2 or excited CS_2* into CS, S, or C (eq 4). In addition, the oxidation reactions for CS_2 with O (or O*) also initiate the CS_2 decomposition (eq 5).[31]

$$Ar + e^- \rightarrow Ar^* + e^- \quad (1)$$

$$O_2 + e^- \text{ (or Ar*)} \rightarrow O_2^* + e^- \text{ (or Ar)} \quad (2a)$$

$$\rightarrow O^* + O \rightarrow O + O \quad (2b)$$

$$O + (e^-, Ar^*) \rightarrow O^* + (e^-, Ar) \quad (3)$$

$$CS_2 + e^- \text{ (or M)} \rightarrow CS_2^* + e^- \text{ (or M)} \quad (4a)$$

$$\rightarrow CS + S \qquad (D_0 = 102.7) \quad (4b)$$

$$CS + e^- \text{ (or M)} \rightarrow C + S \qquad (D_0 = 170.5) \quad (4c)$$

$$CS_2 + O \rightarrow CS + SO$$

$$k_{5a} = 1.734 \times 10^{13} \exp(-650/T) \text{ (cm}^3 \text{ mol}^{-1} \text{ s}^{-1}) \quad (5a)$$

$$CS_2 + O \rightarrow CO + S_2$$

$$k_{5b} = 0.512 \times 10^{12} \exp(-650/T) \text{ (cm}^3 \text{ mol}^{-1} \text{ s}^{-1}) \quad (5b)$$

$$CS_2 + O \rightarrow OCS + S$$

$$k_{5c} = 0.181 \times 10^{12} \exp(-650/T) \text{ (cm}^3 \text{ mol}^{-1} \text{ s}^{-1}) \quad (5c)$$

D_0 in eq 4b,c were the bond dissociation energies in units of kcal/mol, while k_1, k_2, k_3, and k_4 were the reaction rate constants, which were all dependent on the E/p_0 (electric field/reduced pressure) ratio.

In the plasma reactor, the electrons lost part of their kinetic energy because they transferred their energy to the reaction species in high efficiency, but this kinetic energy will be rapidly replenished by the electric field. The charged species such as Ar^+, $O_2^{\pm}$, $O^{\pm}$, $CS_2^{\pm}$, CS^+, S^+, and $S_2^{\pm}$ were also presented in the RF plasma reactor,[32] but their contributions to the reaction processes are negligible.[33] Moreover, the previous study suggested that the ion−molecule reactions could be neglected if the power density was less than 8 W/cm^3.[34,35]

However, Figure 2B illustrates that the power density increased whenever E or R increased, and it was in the range of 0.3−1.0 W/cm^3. Therefore, based on the unselective reactions, consequent transformation of the reactants will produce a great amount of free radicals by sequential self-dissociation or collision with e^- or M (temporary collision partner). The free-radical reactions will be the predominant reactions in this RF system. Besides, when the η_{CS_2} data were compared with the power density, similar profiles were observed. This is because the destruction of CS_2 is mainly via direct electron attack or collision with active species (e.g., Ar*, O, or O*).

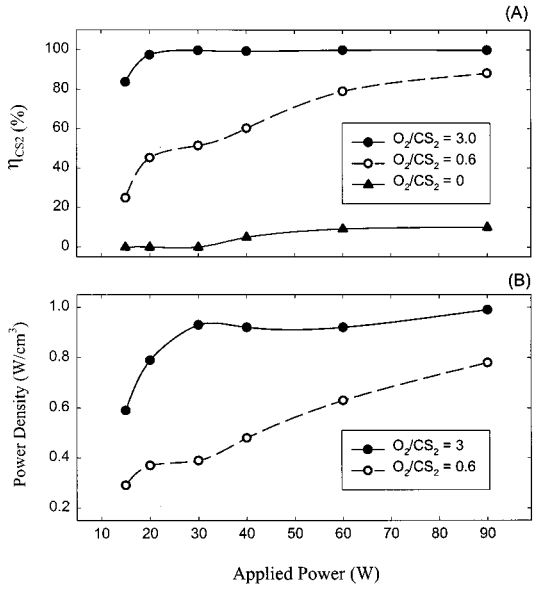

Figure 2. Decomposition fraction of CS_2 (%) (A) and the power density (W/cm^3) (B) affected by various applied powers and O_2/CS_2 ratios.

Table 1. Plasma Operation Conditions and Experimental Results ($CS_{2,in}$ = 5%, Operating Pressure = 30 Torr)

	plasma length (cm)		effluent gas temperature T_g (°C)		gas residence time τ (s)		CS_2 removal efficiency (g/kWh)	
R/E (W)	0.6	3	0.6	3	0.6	3	0.6	3
15	3.8	1.9	51	59	1.02	0.50	16.8	56.8
20	4.1	1.9	63	113	1.05	0.43	23.1	49.6
30	5.7	2.4	80	156	1.40	0.49	17.5	33.8
40	6.2	3.2	108	232	1.42	0.56	15.3	25.3
60	7.0	4.9	172	382	1.37	0.65	13.4	16.9
90	8.4	6.8	386	508	1.11	0.75	10.0	11.3

Operation Conditions. A summary of the plasma operation conditions is shown in Table 1. The plasma lengths ranged from 3.8 to 8.4 cm at $R = 0.6$ and from 1.9 to 6.8 cm at $R = 3.0$, and the effluent gas temperature increased from 51 to 386 °C at $R = 0.6$ and from 59 to 508 °C at $R = 3.0$ as E was increased from 15 to 90 W, respectively. The results reveal that, when the applied power was increased, both plasma lengths and the gas temperature were elevated.

Because of the influence of the gas temperature and plasma physical volume, gas mean residence times (τ) can be computed as a function[36] of plasma length (L) and gas velocity (V) by using the ideal gas expression. The results show that the residence time ranged between 0.43 and 1.42 s (Table 1). Hence, the parallel-connection reactors can be designed with a pair of large parallel electrodes to match the short residence time for industrial application. Therefore, it represents that the power density is a better indicator of η_{CS_2} than of the residence time in the CS_2/O_2/Ar plasma.

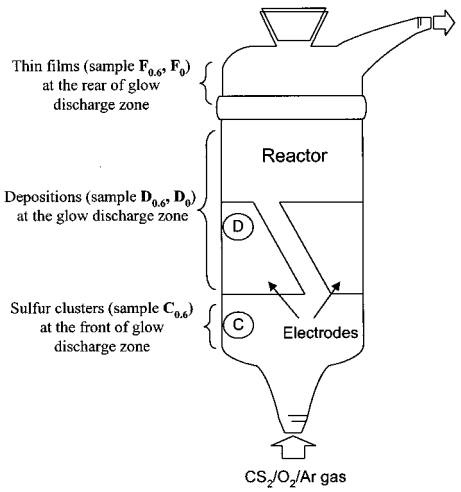

Figure 3. Positions of the solid product.

Table 2. Chemical Analysis Data of Solid Products (mass %)[a]

	$O_2/CS_2 = 0.6$			$O_2/CS_2 = 0$	
elements	sample $C_{0.6}$ (clusters)	sample $D_{0.6}$ (depositions)	sample $F_{0.6}$ (films)	sample D_0 (depositions)	sample F_0 (films)
sulfur	99.24	99.59	83.90	50.70	78.38
carbon	0.14	0.12	11.06	43.39	16.57
oxygen	<0.10	<0.08	3.47	ND	3.59
hydrogen	0.20	0.08	ND	2.31	ND
nitrogen	0.30	0.20	1.57	0.36	1.46
S/C ratio	709:1	832:1	7.59:1	1.17:1	4.73:1

[a] ND: not detectable.

Table 3. Quantification Data for the Fraction of Total Sulfur Input Mass Converted into Effluent Gases (Including Undecomposed CS_2), Thin Films, and Solid Sulfur at the Condition of $R = 0.6$ under Various Applied Powers

applied power (W)	effluent gases (SO_2 + OCS + CS_2) (%)	thin films at the ceiling of the reactor in the rear of the glow discharge zone (%)	solid sulfur (depositions + clusters) (%)
15	87.68	0.74	11.58
20	71.13	1.23	27.63
30	66.68	1.42	31.90
40	56.49	1.55	41.96
60	32.37	1.80	65.84
90	21.23	1.92	76.85

The definition of the removal efficiency (RE_{CS_2}) is the mass of CS_2 decomposed divided by the applied power in an hour (in g/kWh). Table 1 shows that, although a higher RE_{CS_2} was found at $R = 3.0$, no elemental sulfur could be recovered. For $R = 0.6$, the more economic utilization of energy was $RE_{CS_2} = 23.1$ g/kWh at $E = 20$ W; however, the fraction of total input S atoms converted into sulfur was only 27.6% (Table 3). Therefore, a higher applied power is needed, for example, 90 W.

3.2. Solid Product Analysis. Generation of Solid Products. Figure 3 shows the positions of solid products collected. At the condition of $R = 0.6$, large amounts of yellow depositions (called sample $D_{0.6}$) at first were produced in the glow discharge zone around electrodes. Then, the majority of solid depositions were liquidized to form two channels of light-yellow viscous liquid. The liquid flowed along the wall of the reactor from the D zone to the C zone (see Figure 3) and was quenched rapidly to aggregate as solid clusters (called sample $C_{0.6}$). The liquid was generated at the D zone because the wall temperature was about 300 °C around the electrodes so as to fuse the depositions. Then, the liquid cooled down upon reaching the C zone, which was approximately 2−3 cm away from the edge of electrodes and had a lower wall temperature (<120 °C). Hence, $D_{0.6}$ and $C_{0.6}$ were regarded as the same products, and it was difficult to distinguish their differences of amounts.

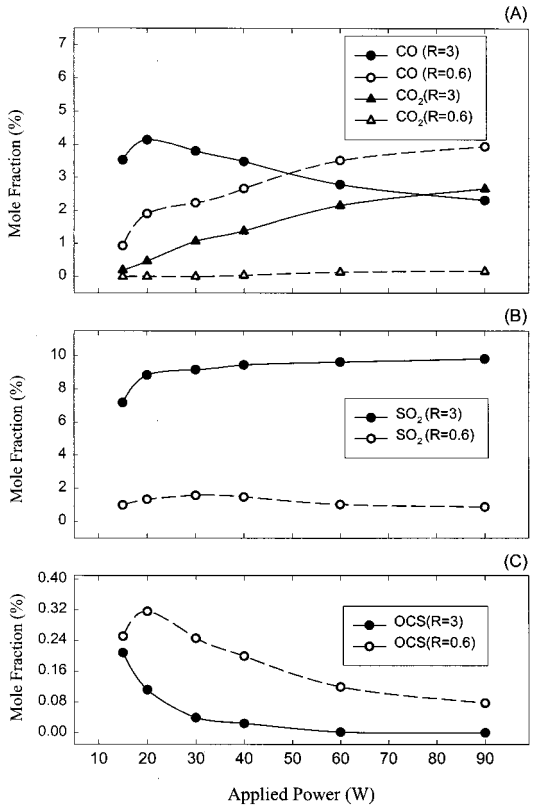

Figure 4. Mole fraction of gaseous products for CO and CO_2 (A), SO_2 (B), and OCS (C) at various applied powers.

For the CS_2/Ar plasma ($R = 0$), small amounts of brown-black solid depositions (called sample D_0) were formed, while no yellow liquids like sample $D_{0.6}$ were observed.

Furthermore, only trace amounts of dark-brown plasma polymeric thin films were collected around the ceiling of the reactor in the rear of the glow discharge zone and called sample $F_{0.6}$ for $R = 0.6$ conditions and sample F_0 for $R = 0$ conditions. The absolute amounts of $F_{0.6}$ or F_0 were far less than those of $D_{0.6}$ or $C_{0.6}$.

Identification of Solid Products. Table 2 lists the results of elemental analysis for solid products and shows that no element sulfur was produced for pure CS_2 decomposition ($R = 0$), while recovery amounts of solid sulfur at the condition of $R = 0.6$ due to the purity of sulfur for the samples $C_{0.6}$ and $D_{0.6}$ reached as high as 99.24% and 99.59%, respectively.

At $R = 0.6$ and with various applied powers, the fraction of total sulfur input mass from CS_2 was converted into three parts, including sulfur-containing effluent gases (SO_2, OCS, and undecomposed CS_2), thin films ($F_{0.6}$), and solid sulfur (depositions $D_{0.6}$ and clusters $C_{0.6}$; Table 3). The results show that the highest yield of solid sulfur and minimum sulfur-containing gases occurred at 90 W and reveal that the amounts of

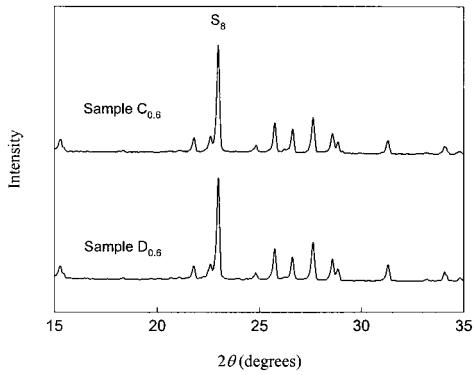

Figure 5. XRD patterns of the sample $C_{0.6}$ and $D_{0.6}$.

both cluster and deposition were far greater than those of the films. In the view of conversion, there was 76.9% of total sulfur input mass converted into solid sulfur in depositions and clusters. The reason was that the elevation of powers led to more activated oxygen to react with C atoms to form CO. These results may provide an approach for sulfur recovery in the solid form to be free of the first process by the hydrogenation of CS_2 to H_2S.

As to the structural characteristics, the XRD patterns of samples $C_{0.6}$ and $D_{0.6}$ possessed high amounts of S_8 (Figure 5), while no apparent single-crystalline structure was observed in the SC-XRD experiments to reveal that the samples were probably of partial amorphous structure. In addition, the samples are easily soluble in CS_2 to indicate that they are not the Sω polymeric sulfur.[37]

At $R = 0$, D_0 was a carbon-rich composition (C/S = 2.28 atom %) because the ionic C or neutral C had a larger diffusivity than that of S or CS to the contribution of heterogeneous wall reactions. Therefore, at $R = 0$, no solid sulfur could be recovered. As for the trace amounts of thin film observed at the conditions of $O_2/CS_2 = 0.6$ and 0, they were not observed at the oxygen-rich conditions. By ESCA, the samples of $F_{0.6}$ and F_0 had sulfur contents corresponding to $CS_{2.84}$ and $CS_{1.77}$, respectively.

3.3. Gaseous Product Distributions. The plasma reactions at $R = 0.6$ and 3.0 were achieved to evaluate the gaseous product distributions. The species detected were SO_2, CO, CO_2, and OCS. The overall reactions in the $CS_2/O_2/Ar$ RF plasma are as follows.

For the oxygen-lean condition ($O_2/CS_2 = 0.6$):

$$CS_2 + O_2 \rightarrow \text{(major) polysulfur, CO, (minor) } SO_2, \text{ (trace) } CO_2, \text{ OCS} \quad (6)$$

For the oxygen-rich condition ($O_2/CS_2 = 3.0$):

$$CS_2 + O_2 \rightarrow \text{(major) } SO_2, CO_2, CO, \text{ (trace) OCS} \quad (7)$$

With increased applied RF power from 15 to 90 W, Figure 4A presents the mole fraction of CO increased from 0.93% to 3.94% for $R = 0.6$ but decreased from 3.53% to 2.31% for $R = 3.0$. At $R = 0.6$, there was not enough oxygen to react completely with CS_2 by the following reaction.

$$CS_2 + 3O_2 \rightarrow CO_2 + 2SO_2$$

At the same range of E, the mole fraction of CO_2 increased from 0% to 0.16% for $R = 0.6$ and from 0.20% to 2.66% for $R = 3.0$. The results show that increased RF power provided a thermodynamically favorable sink for C atoms at the oxygen-lean condition, mainly converted CS_2 into CO, and indicate that the majority of sulfur atoms remained as polysulfur. However, whenever oxygen increased, it was stepwise favored for the formation of CO_2. Figure 4A shows that, at a higher R and a greater E, CO can undergo reaction to CO_2. Furthermore, we observed the similarity of product patterns with oxygen-rich CS_2 flames, but higher yields of CO_2 and a lower gas temperature were found in the $O_2/CS_2/Ar$ RF plasma than in the flame.[5]

OCS was another detected trace product in this study (Figure 4C) that was also observed in previous research such as OH + CS_2 photolysis reaction and CS_2 combustion.[5,38,39] As E increased from 15 to 90 W, the mole fraction of OCS decreased from 0.251% to 0.078% at $R = 0.6$ and from 0.208% to ~0% at $R = 3.0$. The variations indicated that a higher OCS yield took place around an oxygen-lean ($O_2/CS_2 = 0.6$) and a lower applied power (20 W) environment. The reaction for the formation of OCS is probably predominant in eq 5c, while the depletion of OCS was mainly via eq 8.[31]

$$OCS + O \rightarrow CO + SO$$
$$k_8 = 9.632 \times 10^{12} \exp(-2150/T) \text{ (cm}^3 \text{ mol}^{-1} \text{ s}^{-1}\text{)} \quad (8)$$

Only a trace amount of OCS was formed because of a smaller k_{5c}. A weaker OC=S bond (73.3 kcal/mol) and a greater k_8 will make OCS easily dissociated again.

As expected, under the oxygen-rich condition, the predominant sulfur-containing compound was almost invariably SO_2. When E was increased from 15 to 90 W, the mole fraction of SO_2 at first increased from 1.00% to 1.57% and then decreased to 0.87% at $R = 0.6$, while it increased from 7.17% to 9.82% at $R = 3.0$ (Figure 4B). In the oxygen-lean condition, a lower concentration of SO_2 revealed that CO was more oxygen-favored than SO_2. This is due to the higher thermodynamic stability for CO (257 kcal/mol) than OS=O (131.8 kcal/mol) and the greater reaction rate for formation of CO than SO_2. In the viewpoint of conversion, at $E = 90$ W, the fraction of total sulfur input converted into SO_2 only reached 8.75% for $R = 0.6$, while it reached 98.19% for $R = 3.0$.

At $R = 0.6$, the low fraction of total sulfur input converted into SO_2 represented that most of the S atom was not converted into gaseous sulfur-containing species and remained as polysulfur on the wall of reactor. However, the addition of excess oxygen in the CS_2 decomposition resulted in not only the disappearance of OCS but also the generation of a large amount of SO_2.[31,40]

$$O + (S, S_2) = SO + (S) \quad (9a)$$

$$O_2 + S = SO + O$$
$$k_{9b} = 1.30 \times 10^{12} \text{ (cm}^3 \text{ mol}^{-1} \text{ s}^{-1}\text{)} \quad (9b)$$

$$SO + O + M = SO_2 + M$$
$$k_{9c} = 1.1 \times 10^{22} T^{-1.84} \text{ (cm}^6 \text{ mol}^{-2} \text{ s}^{-1}\text{)} \quad (9c)$$

$$SO + SO = SO_2 + S$$
$$k_{9d} = 2.0 \times 10^{12} \exp(-2013/T)\ (\mathrm{cm^3\ mol^{-1}\ s^{-1}}) \quad (9d)$$

For increasing O_2/CS_2 up to 3.0, a part of the electron is attached to O_2; therefore, a large amount of O_2 was dissociated and caused the loss of electron energy.[30] However, the relative density of electrons available for electron impact excitation did not significantly change, and therefore, η_{CS_2} was not affected apparently. In addition, the probability of collision between O, O*, or O_2* and CO was elevated significantly to conduct the increase of conversion of CO into CO_2. Equation 10 shifted to the right-hand side at a higher O_2 concentration, resulting in the reduction of CO attributing to its oxidation to CO_2.[41]

$$CO + O + M = CO_2 + M$$
$$k_{10a} = 5.30 \times 10^{13} \exp(2283.8/T)\ (\mathrm{cm^3\ mol^{-1}\ s^{-1}}) \quad (10a)$$

$$CO + O_2 = CO_2 + O$$
$$k_{10b} = 5.00 \times 10^{13} \exp(-31791/T)\ (\mathrm{cm^3\ mol^{-1}\ s^{-1}}) \quad (10b)$$

From profile patterns similar to those of the CO mole fraction with η_{CS_2} at $O_2/CS = 0.6$ and the SO_2 mole fraction with η_{CS_2} at $O_2/CS_2 = 3.0$, we found that most major product was an indicator of the decomposition efficiency.

The reaction mechanisms for decomposition of CS_2 were built up (Figure 6) and provided useful insight into the formation of SO_2, CO, CO_2, OCS, and polysulfur in the CS_2/O_2/Ar plasma.

In summary, when the products generated through homogeneous and heterogeneous reactions are combined, the overall reaction is presented as follows for the condition of $O_2/CS_2 = 0.6$ at 90 W.

$$CS_2 + 0.6O_2 \rightarrow 1.54/nS_n + 0.83CO + 0.17SO_2 + 0.033CO_2 + 0.015OCS + 0.014CS_{2.84}$$

In practical application, a low concentration of a CS_2-containing gas stream is not suitable for recovering sulfur in the solid form by using a RF plasma system. Low concentration of CS_2 gas can be concentrated by activated carbons and then regenerate these activated carbons to recover sulfur in the solid form.

4. Conclusions

In the oxygen-lean condition ($O_2/CS_2 = 0.6$), 76.9% of total sulfur input mass can be converted into solid sulfur with a purity as high as 99.2% at 90 W, to provide an approach for sulfur recovery from the CS_2-containing gas.

No elemental sulfur was produced for the no-oxygen and oxygen-rich conditions. When O_2/CS_2 was greater than 3.0, the major species detected were SO_2, CO_2, and CO and the trace compound was OCS.

The reaction mechanisms of CS_2 decomposition in the RF plasma environments were built up and revealed that the reaction pathways for the formation of CO and SO_2 involved two main steps: first, CS_2 reacted with e^-, M, O, or O_2 to form CS and OCS; second, the subsequent collisions of CS with O, O_2, or SO rapidly formed CO and SO_2.

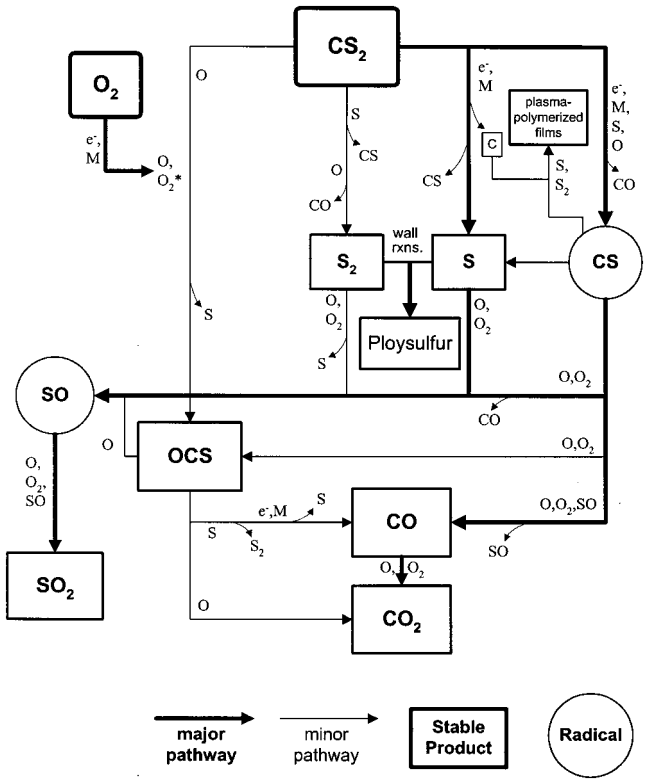

Figure 6. Reaction pathways postulated for the CS_2/O_2/Ar RF plasma.

The optimum conditions were suggested to operate at 90 W in the condition of $O_2/CS_2 = 0.6$ for the feeding gases at room temperature to achieve simultaneously a η_{CS_2} of 88.2%, a removal efficiency of 10.0 g/kWh, and a 76.9% of total sulfur input mass from CS_2 converted into solid sulfur with a low effluent gas temperature (386 °C) in the RF plasma.

Acknowledgment

This research was supported by funds from National Science Council, Taiwan, Grant NSC 90-2211-E-006-048.

Notations

E = applied RF power (W)
R = input O_2/CS_2 molar ratio
τ = gas mean residence time (s)
T_g = effluent gas temperature (K)
η_{CS_2} = CS_2 decomposition fraction (%)
RE_{CS_2}= mass of CS_2 decomposed per unit of applied power per hour (g/kWh)
$CS_{2,in}$ = feed concentration of CS_2 (%)

Literature Cited

(1) Bates, T. S.; Lamb, B. K.; Guenther, A.; Dignon, J.; Stoiber, R. E. Sulfur Emissions to the Atmosphere from Natural Sources. *J. Atmos. Chem.* **1992**, *14*, 315.

(2) Colman, J. J.; Trogler, W. C. Photopolymerization of Carbon Disulfide Yields the High-Pressure-Phase $(CS_2)_x$. *J. Am. Chem. Soc.* **1995**, *117*, 11270.

(3) Alcantara, S.; Estrada, I.; Soledad, V.; Revah, S. Carbon disulfide oxidation by a microbial consortium from a tricking fiber. *Biotechnol. Lett.* **1999**, *21*, 815.

(4) Ghittori, S.; Maestri, L.; Contardi, I.; Zadra, P.; Marraccini, P.; Imbriani, M. Biological Monitoring of Workers Exposed to Carbon Disulfide (CS_2) in a Viscose Rayon Fibers Factory. *Am. J. Ind. Med.* **1998**, *33*, 478.

(5) Cullis, C. F. The Kinetics of Combustion of Gaseous Sulphur Compounds. *Combust. Flame* **1972**, *18*, 225.

(6) Li, C. T.; Lee, W. J.; Chen, C. Y.; Wang, Y. T. CH_2Cl_2 Decomposition by Using a Radio-Frequency Plasma System. *J. Chem. Technol. Biotechnol.* **1996**, *66*, 382.

(7) Hsieh, L. T.; Lee, W. J.; Chen, C. Y.; Wu, Y. P. G.; Chen, S. J.; Wang, Y. F. Decomposition of Methyl Chloride by Using an RF Plasma Reactor. *J. Hazard. Mater.* **1998**, *63*, 69.

(8) Wang, Y. F.; Lee, W. J.; Chen, C. Y. Decomposition of Dichlorodifluoromethane by adding Hydrogen in a Cold Plasma System. *Environ. Sci. Technol.* **1999**, *33*, 2234.

(9) Wang, Y. F.; Lee, W. J.; Chen, C. Y. Reaction Mechanisms in Both a CHF_3/O_2/Ar and CHF_3/H_2/Ar Radio Frequency Plasma Environment. *Ind. Eng. Chem. Res.* **1999**, *38*, 3199.

(10) Liao, W. T.; Lee, W. J.; Chen, C. Y.; Hsieh, L. T.; Lai, C. C. Decomposition of ethoxyethane in the cold plasma environment. *J. Chem. Technol. Biotechnol.* **2000**, *75*, 817.

(11) Liao, W. T.; Lee, W. J.; Chen, C. Y.; Shih, M. Decomposition of ethylene oxide in the RF plasma environment. *Environ. Technol.* **2001**, *22*, 165.

(12) Miller, G. P.; Baird, J. K. Radio Frequency Plasma Decomposition of Ammonia: A Comparison with Radiation Chemistry Using the *G* Value. *J. Phys. Chem.* **1993**, *97*, 10984.

(13) Teimurova, F. A.; Rasulov, A. M.; Klimov, N. T. Hydrogen Sulfide Dissociation in a Barrier Discharge Plasma. *High Energy Chem.* **1992**, *25*, 316.

(14) Nester, S. A.; Rusanov, V. D.; Fridman, A. A. Dissociation of Hydrogen Sulfide in a Plasma Containing a Small Amount of Oxygen. *High Energy Chem.* **1989**, *22*, 389.

(15) Chang, M. B.; Balbach, J. H.; Rood, M. J.; Kushner, M. J. Removal of SO_2 from Gas Streams Using a Dielectric Barrier Discharge and Combined Plasma Photolysis. *J. Appl. Phys.* **1991**, *69*, 4409.

(16) Eliasson, B.; Kogelschatz, U. Nonequilibrium Volume Plasma Chemical Processing. *IEEE Trans. Plasma Sci.* **1991**, *19*, 1063.

(17) Fgoli, N. S.; L'Argentire, P. C.; Nicot, C.; Frty, R. Regeneration of Ni/SiO_2 poisoned with Carbon Disulfide. *Catal. Lett.* **1996**, *38*, 171.

(18) Raymont, M. E. D. *Sulfur: New Sources and Uses*; ACS Symposium Series 183; American Chemistry Society: Washington, DC, 1982.

(19) Walley, E. Structure of Bridgman's Black Carbon Disulphide. *Can. J. Chem.* **1960**, *38*, 2105.

(20) Chan, W. S.; Jonscher, A. K. Structural and Electrical Properties of Solid Polymeric Carbon Disulphide. *Phys. Status Solidi* **1969**, *32*, 749.

(21) Tsukamoto, J.; Takahashi, A. Polymeric Product of Carbon Disulfide and Its Electrical Properities. *Jpn. J. Appl. Phys.* **1986**, *25*, L338.

(22) De Sorgo, M.; Yarwood A. J.; Strausz, O. P.; Gunning, H. E. The Photolysis of Carbon Disulfide and Carbon Disulfide−Oxygen. *Can. J. Chem.* **1965**, *43*, 1886.

(23) Ernst, K.; Hoffman, J. J. Laser Induced Aerosol Formation in CS_2 Vapour. *Chem. Phys. Lett.* **1979**, *68*, 40.

(24) Matsuzaki, A.; Hamada, Y.; Morita, H.; Matsuzaki, T. Raman and Infrared Spectra of Sediments in Laser-induced Aerosol Formation from CS_2 Vapor. *Chem. Phys. Lett.* **1992**, 337.

(25) Desai, S. R.; Feigerle, C. S.; Miller, J. C. Laser-Induced Polymerization within Carbon Disulfide Clusters. *J. Phys. Chem.* **1995**, *99*, 1786.

(26) Van Drumpt, J. D. Polymer Formation from Carbon Disulfide in a Silent Electrical Discharge. *Int. J. Sulfur Chem.* **1972**, *2*, 291.

(27) Hirotsu, T. Plasma Reaction Behavior of Carbon Disulfide and Carbon Dioxide in Glow Discharges. *J. Macromol. Sci., Chem.* **1981**, *A16* (7), 1217.

(28) Asano, Y. Formation and Properties of Plasma-Polymerized Carbon Disulfide Films. *Jpn. J. Appl. Phys.* **1983**, *22*, 1618.

(29) Boenig, H. V. *Fundamentals of Plasma Chemistry and Technology*; Technomic Publishing Co., Inc.: Lancaster, PA, 1988.

(30) Rauf, S.; Kushner, M. J. Argon metastable densities in radio frequency Ar, Ar/O_2 and Ar/CF_4 electrical discharges. *J. Appl. Phys.* **1997**, *82*, 2805.

(31) Atkinson, R.; Baulch, D. L.; Cox, R. A.; Hampson, R. F., Jr.; Kerr, J. A.; Rossi, M. J.; Troe, J. Evaluated Kinetic and Photochemical Data for Atmospheric Chemistry. *J. Phys. Chem. Ref. Data* **1997**, *26*, 1329.

(32) Hiraoka, K.; Fujimaki, S.; Aruga, K. Frontier-Controlled Structures of the Gas-Phase $A^{\pm}(CS_2)_n$ Clusters, $A^{\pm} = S_2^+$, CS_2^+, S_2^-, and CS_2^-. *J. Phys. Chem.* **1994**, *98*, 1802.

(33) Bains-Sahota, S. K.; Thiemens, H. Mass-Independent Oxygen Isotopic Fractionation in a Microwave Plasma. *J. Phys. Chem.* **1987**, *91*, 4370.

(34) Brown, L. C.; Bell, A. T. Kinetics of the Oxidation of Carbon Monooxide and the Decomposition of Carbon Dioxide in a Radiofrequency Electric Discharge. I. Experimental Results. *Ind. Eng. Chem. Fundam.* **1974**, *13*, 203.

(35) Bozzelli, J. W.; Barat, R. B. Reactions of Water Vapor or Molecular Hydrogen with Trichloroethylene in a Microwave Plasma Reactor. *Plasma Chem. Plasma Process.* **1988**, *8*, 293.

(36) Arno, J.; Bevan, J. W. Detoxification of Trichloroethylene in a Low-Pressure Surface Wave Plasma Reactor. *Environ. Sci. Technol.* **1996**, *30*, 2427.

(37) Van Miltenburg, J. C.; Fourcade, J.; Ezzine, M.; Bergman, D. Thermodynamic Properties of Polymeric Sulfur $S\omega_2$ at temperatures between 5K and 370K. *J. Chem. Thermodyn.* **1993**, *25*, 1119.

(38) Barnes, K. H.; Becker, E. H.; Fink, A.; Reimer, A.; Zabel, F. Rate Constants and Products of the Reaction $CS_2 + OH$ in the Pressure of O_2. *Int. J. Chem. Kinet.* **1983**, *15*, 631.

(39) Lovejoy, E. R.; Murrells, T. P.; Ravishankara, A. R.; Howard, C. J. Oxidation of CS_2 by Reaction with OH. 2. Yields of HO_2 and SO_2 in Oxygen. *J. Phys. Chem.* **1990**, *94*, 2386.

(40) Glarborg, P.; Kubel, D.; Dam-Johnson, K.; Chiang, H. M.; Bozzelli, J. W. Impact of SO_2 and NO on CO oxidation under Post-Flame Conditions. *Int. J. Chem. Kinet.* **1996**, *28*, 773.

(41) Karra, S. B.; Senkan, S. M. A Detailed Chemical Kinetic Mechanism for the Oxidative Pyrolysis of CH_3Cl. *Ind. Eng. Chem. Res.* **1988**, *27*, 1163.

Received for review March 29, 2001
Revised manuscript received July 24, 2001
Accepted December 29, 2001

IE010292S